

Femtosecond Polarized Pump–Probe and Stimulated Emission Spectroscopy of the Isomerization Reaction of Rhodopsin

Gilad Haran,^{†,‡} Elisabeth A. Morlino,^{†,‡} Jens Matthes,[§] Robert H. Callender,[§] and Robin M. Hochstrasser^{*,†}

Department of Chemistry, University of Pennsylvania, Philadelphia, Pennsylvania 19104, and Department of Biochemistry, Albert Einstein College of Medicine, The Bronx, New York 10461

Received: August 5, 1998; In Final Form: October 22, 1998

The isomerization reaction of retinal in bovine rhodopsin was studied by femtosecond optical techniques. Probing at near-IR wavelengths allowed detection of stimulated emission, the rise and decay of which was too fast to be resolved with our 70 fs pulses. The fast dynamics of the emission suggest a multidimensional potential energy surface for isomerization, possibly involving carbon double-bond stretching in addition to bond torsion, as previously invoked for model systems by quantum mechanical calculations. A polarized pump–probe measurement of the appearance of the first isomerization product, bathorhodopsin, at 580 nm shows that the initial direction of the retinal electronic transition dipole moment in this product could be as much as 30° away from the original direction, as deduced from an anisotropy of 0.25. If this is the case, there would need to be significant electronic changes and charge translocations accompanying the reaction. The anisotropy settles, with an exponential fit time constant of $6.0 \pm 0.6 \times 10^{12} \text{ s}^{-1}$, to a value of 0.34 ± 0.01 , corresponding to an angle of 16.5°. Coherent vibrational oscillations in the product well are shown to involve reorientations of the transition dipole direction of less than 4°. A new transient absorption at ca. 700 nm was discovered and attributed to unreactive rhodopsin. The results presented here provide new benchmarks for theoretical evaluation of the isomerization mechanism and dynamics in rhodopsin.

Introduction

The first step in the photochemical reaction cascade of the visual protein rhodopsin involves isomerization of the retinal cofactor in the protein from an 11-cis to an all-trans form.¹ The retinal is located in a region of the protein termed the “retinal pocket”. It is covalently attached as a protonated Schiff base (PSB) to the side chain of lysine-296, where in bovine rhodopsin, the protonated Schiff base linkage end of retinal is “anchored” into position by its negatively charged counterion, glutamate-113.^{2–4} There are several key changes in the photochemical properties of the retinal chromophore as it binds in the retinal pocket. In the first place, the photoisomerization is very efficient in rhodopsin compared to in solution; it has a higher quantum yield (0.67 vs 0.15) and occurs much faster.⁵ The potential energy surface along the torsional (isomerization) coordinate is dramatically changed. In solution, the energy difference between 11-cis and all-trans ground-state retinal is less than 1 kcal/mol and there is an excited-state barrier to isomerization. The one-dimensional representation of the free energy surfaces for rhodopsin isomerization is shown in Figure 1. Contrary to the case of retinal in solution, the difference in energy from cis to trans forms is now some 35 kcal/mol, the energy barrier for the ground-state isomerization is much higher, and the excited-state isomerization is now barrierless. It is believed that some combination of electrostatic and steric interactions between the bound retinal chromophore and the apoprotein are responsible for these differences. In any case,

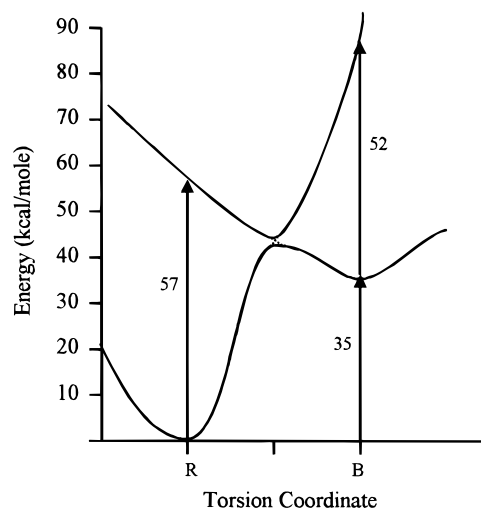


Figure 1. One-dimensional potential energy surface for 11-cis to all-trans isomerization in rhodopsin. R = rhodopsin, B = bathorhodopsin.^{35,36} The known free energy differences are indicated in kcal/mol.

the protein guides the retinal excited-state population preferentially along the pathway leading to isomerization. A similar effect in bacteriorhodopsin was termed “protein catalysis” by Song et al.⁶

Mathies, Shank, and co-workers^{7,8} showed that the absorption spectrum of a productlike species of bovine rhodopsin is formed in 200 fs. The equilibrated trans photoproduct, bathorhodopsin, is formed on the 3 ps time scale.^{7–9} The fluorescence quantum yield of rhodopsin ($\sim 10^{-5}$) corresponds to an excited-state lifetime of ~ 50 fs.^{10,11} The excitation wavelength dependence of the fluorescence spectrum indicates that the fluorescence

* To whom correspondence should be addressed. E-mail: hochstra@sas.upenn.edu. Fax: 215-898-0590.

[†] University of Pennsylvania.

[‡] These authors contributed equally to this work.

[§] Albert Einstein College of Medicine.

arises mainly from vibrationally unrelaxed configurations of the molecules.¹¹ Stimulated emission of the fluorescent state of native rhodopsin was not detected in previous femtosecond pump–probe studies.⁸ The presence of fluorescence and absence of stimulated emission in pump–probe absorption experiments presents an interesting paradox. A similar situation arose in the case of bacteriorhodopsin where the absence of stimulated emission was ultimately shown to be caused by the presence of an induced absorption in the gain region.^{12,13}

On the basis of the extremely high speed of the reaction, as well as on the observation of vibrational coherence in the product,¹⁴ it has been proposed that the reactive motion involves Landau–Zener-type curve-crossing from the first excited state of the 11-*cis* molecule (S_1) to the ground state of the all-*trans* product (S_0). Recent *ab initio* calculations by Garavelli et al.^{15–17} on two isolated protonated Schiff base models for retinal photoisomerization suggest that at the crossing point the S_0 and S_1 surfaces are actually degenerate, forming a conical intersection. The calculations also show that the isomerization in model systems is a multidimensional process where the first changes in nuclear coordinates after excitation are the stretching of the double bond to be isomerized and its two neighboring double bonds.^{15–17} This motion leads to a free energy decrease without substantial development of torsion in the isomerizing bond. A similar process was earlier predicted by Warshel¹⁸ and recently indicated by femtosecond pump–probe measurements on bacteriorhodopsin.^{12,19} Quantum mechanical calculations^{15–17,20,21} further suggest that the rapid nuclear motion is accompanied by changes in the charge distribution, amounting to motion of a positive charge away from the Schiff base end of the retinal. The torsional motion is suggested to occur essentially after these faster processes are completed.

The picture can be even more complex than that suggested by model calculations when taking into account that the isomerization takes place inside a protein. Geometrical constraints restrict the possible motions, and there could be significant energy penalties associated with following the reaction path of the isolated molecule. Thus, there can be no large-scale nuclear motions accompanying isomerization in the protein. Instead, it is possible that the retinal cofactor overcomes this by developing torsion in the double bonds adjacent to the isomerizing bond.^{22,23} Furthermore, electrostatic effects or proton-transfer steps accompanying isomerization^{18,20,24} can also lead to potential energy surfaces that are very different from those of the isolated molecule.

In the present work, the wavelength range of earlier sub-50 fs studies^{7,8} was extended into the near-infrared by conducting pump–probe experiments from 600 to 900 nm. The anisotropy of the pump–probe signal from the nascent all-*trans* product shows significant evolution, which may imply electronic relaxation accompanying isomerization or there may be new absorbing transients at the monitoring wavelength. Motion on the excited-state surface *preceding* curve-crossing was identified from the time profile of stimulated emission and transient absorption at near-IR wavelengths.

Experimental Section

Bovine rod outer segments were isolated from frozen retinas by the sucrose step-gradient method.²⁵ Samples were washed with 10 mM HEPES in H_2O and then solubilized in 20 mM *n*-dodecyl maltoside/0.1 M hydroxylamine/10 mM HEPES, adjusted to pH 7.0. The final sample had an optical density of $\sim 5/\text{cm}$ at 500 nm. The ratio of protein absorption at 280 nm to retinal absorption at 500 nm (<3) served as a test for the intactness of the sample before measurements.

A home-built Ti:sapphire regenerative amplifier was used to produce 50 fs, 250 μJ pulses centered at 810 nm, at a repetition rate of 1 kHz. A 500 nm pump source was parametrically generated from the 810 nm source using a dual stage optical parametric amplifier, each stage utilizing 50% of the light. In the first stage, 10% of the 810 nm light was used to produce a white light continuum, which was then recombined collinearly with the residual 810 nm light on a 2 mm type II BBO crystal. The crystal was double-passed to produce $\sim 10 \mu\text{J}$ of infrared light. In the second stage, the infrared light was separated from the remaining 810 nm light and focused on a 0.5 mm type I BBO crystal jointly with a “fresh” 810 nm beam to produce visible light by sum frequency generation. A 10 nm bandwidth interference filter was used to spectrally select the generated light at 500 nm; the power measured through the filter was 300–400 nJ. A small portion of the 810 nm beam was used for a probe, either directly (after proper attenuation) or by focusing it on a 2 mm sapphire window to generate a white light continuum, a spectral slice of which was selected with an interference filter. Cross-correlation of the pump pulse with the 810 nm probe pulse was 100 fs fwhm, while the cross-correlation with the white light continuum probe pulse (at 580 nm) was 140 fs fwhm.

The rhodopsin sample was flowed through a 0.5 mm optical path cell equipped with 1 mm thick quartz windows. Part of the probe beam was split before the sample and sent to a silicon photodiode to serve as a reference. The rest was focused in the sample using a 5 cm lens. The pump beam was focused using a 25 cm lens, to generate a bigger spot than the probe beam, and the two were overlapped in the sample. The probe beam was detected after the sample with a second silicon photodiode, the signal of which was normalized to the reference photodiode signal on a shot-to-shot basis. The pump pulse train was mechanically chopped at half the laser repetition rate, and relative absorbance changes were calculated from each pair of chopped/unchopped photodiode signals and averaged over a few thousand pairs. The time delay between the pump and probe beams was varied using a motorized optical delay line inserted in the probe path.

In the anisotropy experiments, the pump beam polarization direction was changed intermittently between parallel and perpendicular with respect to the vertically polarized probe beam. This allowed us to avoid any systematic errors in the anisotropy measurement due to the gradual drop in the rhodopsin signal that follows permanent photobleaching. The experimental anisotropy function was obtained from the measured signals using the well-known relation

$$r(t) = \frac{I_{\parallel}(t) - I_{\perp}(t)}{I_{\parallel}(t) + 2I_{\perp}(t)}$$

where $I_{\parallel}(t)$ and $I_{\perp}(t)$ are the parallel and perpendicular signals, respectively, and the denominator is the isotropic or “magic-angle” signal. No more than 100 nJ of pump pulse energy was used for the anisotropy experiments. At this energy level, 5–7.5% of the sample at the focus of the pump beam was excited by each laser shot. The required anisotropy correction (0.01) for this small but finite bleach is taken into account in all of the values quoted herein. A pulse energy of 200–300 nJ was used in the remainder of the experiments.

Results

Anisotropy at 580 nm. Recirculated bovine rhodopsin samples were excited close to the maximum of the $S_0 \rightarrow S_1$

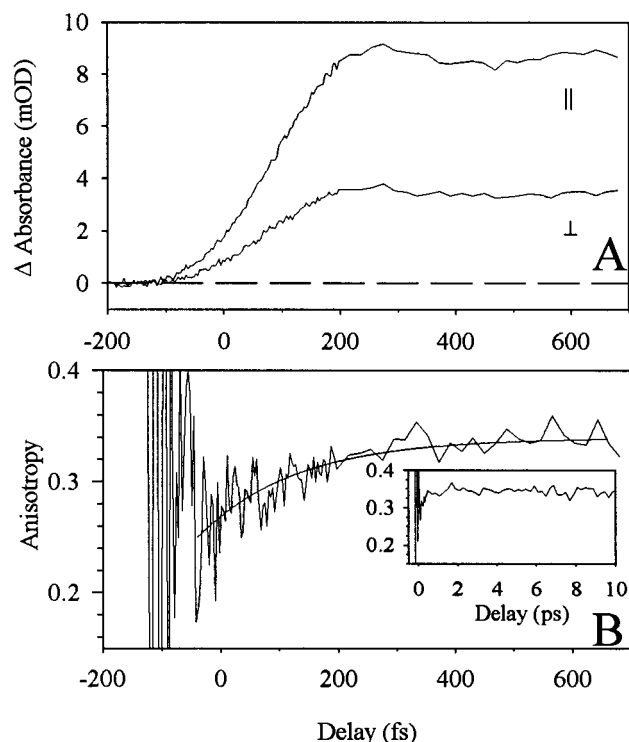


Figure 2. Polarized 500 nm pump/580 nm probe measurement of rhodopsin: (A) the experimental signals, obtained with the pump and probe beams polarized parallel (||) or perpendicular (⊥) to each other; (B) the anisotropy function calculated from the signals. The fit is from a simulation involving changing electronic wave functions as isomerization proceeds described more fully in the text. The inset shows a long time (10 ps) scan of the anisotropy, from a separate experiment. It is seen that after ~ 300 fs there is no further change in the anisotropy value from 0.34 ± 0.01 .

absorption band (R in Figure 1), while a 580 nm probe wavelength was selected to detect bathorhodopsin formation close to the maximum of this product's $S_0 \rightarrow S_1$ absorption band at early times⁸ (B in Figure 1). The experimental signals are shown in Figure 2A. The anisotropy function, calculated from the same signals, is shown in Figure 2B. At negative pump–probe delays, the anisotropy function fluctuates wildly, as expected for vanishingly small experimental signals. At positive delays, however, the anisotropy is well determined by the data and exhibits a rise with a rate constant of $6.0 \pm 0.5 \times 10^{12} \text{ s}^{-1}$ from a value of approximately 0.25 near delay time zero to a final value of 0.34. These data also suggest that the rise of the anisotropy is preceded by a rapid decay. However, the signal-to-noise ratio for negative delays is inadequate to establish unequivocally the presence of this decay so it will not be discussed further. The inset shows the anisotropy obtained from a separate experiment where the pump–probe delay time was scanned up to 10 ps. It shows that after the initial rise, the anisotropy function remains constant over this period with an average value of 0.34 ± 0.01 . Thus, the only observable change in the anisotropy in our experiment occurs during the first 400 fs.

New Transient Absorption. Figure 3 shows the signals, normalized to unit change in optical density, obtained from exciting rhodopsin samples with 500 nm pulses and probing at various wavelengths between 600 and 750 nm. At all these probe wavelengths, a rapid rise in absorbance is seen that we refer to as the excited-state absorption. This contribution to the signal grows as the wavelength is increased, while that of the product state absorption, dominating at 600 nm, decreases. At some

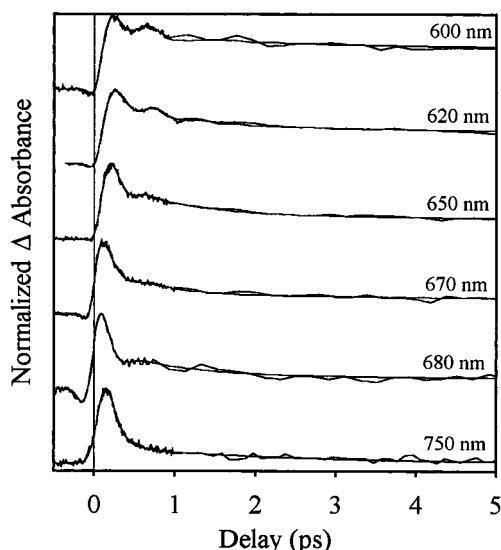


Figure 3. Kinetic profiles of 500 nm pumped rhodopsin. Monitoring wavelengths are shown in the figure. All of the signals were normalized to unit change in optical density. The sample concentration was depleted by differing amounts of photodegradation during the data acquisitions. The actual signals were approximately in the ratios 1.0:0.75:0.57:0.43:0.38:0.24 in order of increasing wavelength. The pump and probe beams were polarized parallel.

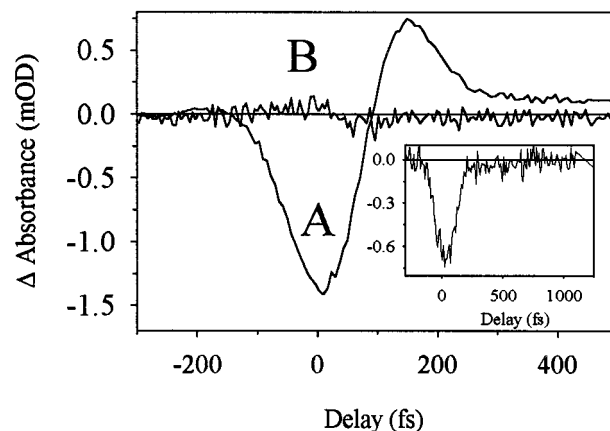


Figure 4. Instrument-response-limited stimulated emission detected in a 500 nm pump/810 nm probe measurement of rhodopsin (A). Response of a bleached rhodopsin sample (B). The inset displays the stimulated emission signal detected at 900 nm.

probe wavelengths (600, 620, 670, and 680 nm) a gain signal is seen initially that is soon overcome by the absorbance. All of the data fit to a model with a fast gain component, rising and decaying with a lifetime of < 50 fs (see below), an excited-state absorption, and a product-state absorption. The decay of the excited-state absorption varied with wavelength. The data fitted approximately to an exponential with a lifetime of 0.64 ± 0.05 ps at wavelengths less than 650 nm, and 0.12 ps for wavelengths greater than 650 nm.

Stimulated Emission. The signal obtained by pumping rhodopsin samples at 500 nm and probing at 810 nm is shown in Figure 4 (trace A). Similar signals but with differing amplitudes were observed throughout the spectral region between 800 and 900 nm. The signal obtained at 900 nm is shown as an inset. The rise and fall of the stimulated emission part of these signals are both instrument response limited at less than 40 fs. An absorptive signal remains after the decay of the emission at 810 nm. The nature of this transient absorption is unknown. The data are consistent with a model in which the

stimulated emission and absorption are present immediately and decay with differing rate constants.

Also shown in Figure 4 (trace B) is the signal obtained from a photochemically degraded rhodopsin sample. The absence of a significant signal from this sample indicates that the stimulated emission signal is from rhodopsin and not any products formed upon photolysis. Neither are those gain signals due to contributions from nonlinear coupling of the fields. All spectral filtering in the experiment was done *before* the sample, and all transmitted frequency components of the pulses were detected.

Discussion

The data presented in this paper shed new light on the mechanism and the potential energy surfaces involved in the cis-trans isomerization of rhodopsin. Motion away from the Franck-Condon region on the excited-state surface is reflected in the stimulated emission measurement, and new aspects of motion in the ground-state well of the product bathorhodopsin after curve-crossing are suggested by the time-dependent anisotropy.

The stimulated emission of Figure 4 shows instrument response-limited rise and decay. If the reaction coordinate were represented by Figure 1, one would expect the fluorescence to shift to lower energy and a significant rise time on the emission signal as the system moves to the crossing point of the rhodopsin and bathorhodopsin surfaces. The absence of such a rise time in our data shows that any dynamic Stokes shift of the emission spectrum is extremely fast (as noted above, faster than 40 fs). The picture of a reaction coordinate as in Figure 1 is therefore missing an essential part of the dynamics. Such a fast Stokes shift must involve high-frequency vibrational modes. Obvious candidates are the carbon-carbon stretches. The similarity of this situation to the one suggested to explain the bacteriorhodopsin experiments^{12,19} is striking, and both results suggest that bond stretching is an important first step preceding isomerization. The fast decay of the stimulated emission suggests that in bovine rhodopsin the initial population is driven out of the 11-cis Franck-Condon region in a time that is faster than the torsional motion along the coordinate of Figure 1. However, the photogenerated population must reside on an excited-state surface for ca. 200 fs corresponding to the time for the appearance of the product absorbing at 580 nm.⁸ Thus, the stimulated emission reports on the initially excited state but lacks information concerning large parts of the nuclear or electronic motions that occur between the Franck-Condon region and the curve-crossing with the product well. This differs from the situation with octopus rhodopsin²⁶ where a significant fraction of the generated excited states continue to emit for several picoseconds. Kandori et al. in their fluorescence up-conversion study, at a time resolution of 60 fs, of a rhodopsin analogue containing an eight-membered ring retinal,²⁷ were unable to detect any rise in their fluorescence signals at long wavelengths, which is also consistent with there being a fast Stokes shift in that case.

The data in Figure 3 report on a new transient absorption band at wavelengths around 700 nm. This absorption appears faster than our time resolution and decays within 800 fs. This absorption might represent the population that does not isomerize, since it is present before and after the 580 nm product is formed. The residual absorbances seen in Figure 3 are due to the tail of the bathorhodopsin absorption band centered at 580 nm.²⁵ The decay of this residual signal was attributed to the vibrational cooling of bathorhodopsin.^{7,8} Preliminary transient spectra, assembled directly (without deconvolution) from ex-

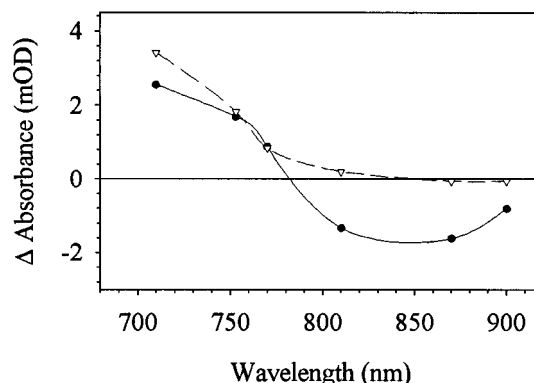


Figure 5. Transient spectra of rhodopsin, excited at 500 nm, assembled from signals obtained by probing at different wavelengths. The solid line is at approximately 4 fs, and the dashed line is at approximately 250 fs.

perimental signals obtained at various near-IR wavelengths, are shown in Figure 5. The spectrum at the earliest time shows the net absorption appearing at 700–720 nm and the net gain apparently centered at approximately 840 nm. At times later than ca. 250 fs, the stimulated emission is gone but some absorption, now due only to bathorhodopsin, still remains.

The measurement of the polarization anisotropy at 580 nm provides information about the evolution of the transition dipole direction of the forming bathorhodopsin. The earliest anisotropy value obtained with confidence in our measurement is 0.25, which rises to a final value of 0.34. This initial process is 90% completed in 385 fs. From the relation $r = 2/5(P_2(\cos \theta))$, where θ is the angle between pumped and probed transitions and P_2 is the second Legendre polynomial, this anisotropy would correspond to a θ of 30°. The anisotropy of $r = 0.34$ at later times, after correction for partial saturation, would correspond to $\theta = 16.5^\circ$. These would be the angular changes of the transition dipole needed to explain the anisotropy. However, the time-dependent anisotropy at early times can be explained in two ways. One involves rotation of the transition dipole due to either nuclear or electronic dynamics accompanying the isomerization reaction. The other requires overlapping retinal transitions (see below).

Concerning rotation of the transition dipole, no large-scale nuclear motions are expected during the initial isomerization reaction in rhodopsin.^{22,23} Furthermore, such a large nuclear displacement would be expected to take considerably more time than the less than 40 fs that is available (see above). Therefore, it seems unlikely that a transition dipole reorientation of 30° could be interpreted as an angular nuclear motion of the retinal backbone structure. An effect involving a change in the electronic wave functions seems more likely. A significant rotation of the electronic transition dipole moment could arise very quickly if there were a sudden charge movement accompanying excitation, even if the nuclei were not much displaced. This interpretation invokes the occurrence of significant changes in the electronic wave functions that could be investigated by theoretical calculations. As the molecule undergoes motion along the torsion coordinate, the electronic transition dipole recovers to be within 16.5° of its original direction in 11-cis at 500 nm.

The alternative interpretation for the anisotropy changes involves the overlapping of several different time-dependent transients. While 580 nm is the wavelength of the absorption maximum of bathorhodopsin at early times,⁸ there can be other contributions to the signal at this probe wavelength. The fluorescence spectrum of rhodopsin peaks at 650 nm, and its

intensity is half of the maximum at 580 nm.¹¹ Therefore, there should be a stimulated emission signal at 580 nm appearing instantaneously and decaying as the motion on the excited-state surface causes the nuclei to leave the FC region. The stimulated emission having these characteristics was most prominent at wavelengths greater than 800 nm. No net stimulated emission is seen at 580 nm or at any other wavelength in the range probed by Peteanu et al. (470–670 nm).⁸ One explanation for the lack of stimulated emission is that it is canceled by a transient absorption at 580 nm. If the transient excited-state absorption signal that putatively cancels the stimulated emission at zero delay time were to have low anisotropy, then the total signal would also show low anisotropy.²⁸ As the excited-state absorption and the stimulated emission decay, the isomerization reaction product anisotropy would be recovered. Using this idea, we tried to develop a model that fits the anisotropy results obtained at 580 nm. The magnitude of the expected stimulated emission signal that should be present in the 580 nm data was estimated from the stimulated emission signal at 810 nm and the known fluorescence spectrum.¹⁹ The proportions of stimulated emission and bathorhodopsin absorption were estimated from the known extinction coefficients of bathorhodopsin and rhodopsin²⁹ and the fluorescence spectrum.¹¹ The stimulated emission signal at 580 nm was assigned an anisotropy of 0.4. The anisotropy of the bathorhodopsin absorption was assigned the value 0.34 determined from the long-time anisotropy data (inset Figure 2B). Using these parameters, a reasonable fit to the experimental signals at 580 nm required the presence of a transient absorption with an anisotropy of -0.1 and a lifetime of ca. 250 fs, considerably longer than the stimulated emission lifetime. When the model response function obtained from the fit was convoluted with a 35 fs pulse a discernible initial emissive signal is predicted. Such a signal was not detected in the experiment by Peteanu et al.⁸ Although the expected effects of stimulated emission are quite small, this argues against the model including transient absorption and stimulated emission. An anisotropy of -0.1 corresponds to $\theta = 66^\circ$. This is a large angle considering most strong transitions of retinal are polarized in directions close to their longest conjugated axis. However, there are reports of so-called *cis* bands with transition dipole moments deviating significantly from this axis,^{30–33} so the angle alone does not definitely exclude the occurrence of a depolarized transient absorption. Therefore, our experiments do not exclude the possibility that the anisotropy rise is caused by an underlying excited-state absorption.

After its initial rise, the anisotropy at 580 nm stays constant (at a value of 0.34 ± 0.01) for at least 10 ps. This is in contrast to the signals themselves, which contain an oscillation with a period of 550 fs. This oscillation was first seen by Wang et al.¹⁴ who attributed it to coherent vibrational motion of a torsional mode associated with the isomerization process. The modulation depth of the oscillation in Figure 2A is consistent with the experiment of Wang et al. when adjustment for the different pulse width of laser pulses utilized in the two experiments is incorporated. The oscillation is absent in the anisotropy data, indicating that the coherent motion leading to the signal oscillation does not significantly change the direction of the $S_0 \rightarrow S_1$ transition dipole moment of the product. In fact, according to our experiments, the 550 fs oscillatory motion of this wave packet cannot be accompanied by more than a 4° angular motion of the electronic transition dipole.

The longer time anisotropy value is significantly lower than 0.4, the expected value for the anisotropy of pumped and probed transitions with parallel transition dipole moments. The transition

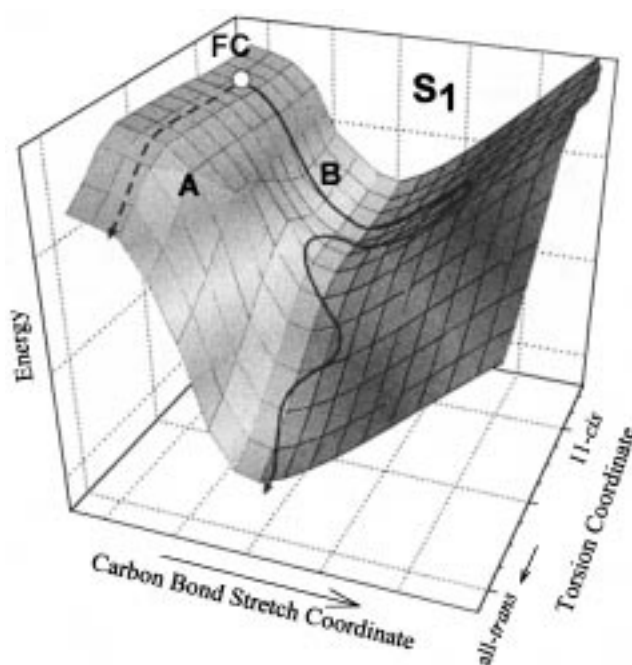


Figure 6. Two-dimensional potential energy surface pictorially describing the initial motions of retinal after excitation. Path A shows the traditional deactivation pathway, involving motion only along the torsion coordinate. Path B shows the deactivation pathway proposed herein, involving carbon bond stretching preceding torsional motion as the excited-state population approaches the S_1/S_0 crossing point.

dipole moment direction of retinal in bathorhodopsin at ~ 400 fs is clearly tilted from the transition dipole moment direction in rhodopsin, and the tilt angle is calculated to be $16.5 \pm 2^\circ$. There were several previous investigations of the change in the transition dipole direction of retinal in bathorhodopsin compared with rhodopsin, which agree quite well with our result. The values included $\theta = 8 \pm 2^\circ$, from linear dichroism measurements at 10 ns in bovine rhodopsin,³⁴ $11 \pm 3^\circ$, from static polarized absorption and linear dichroism measurements at low temperatures in frog rhodopsin,³² and 26° , also from static polarized absorption at low temperatures in frog rhodopsin.^{30,31}

Conclusion

In summary, we have used polarized pump–probe spectroscopy to monitor the changes in the transition dipole direction during the initial isomerization reaction of bovine rhodopsin. We found that the electronic transition dipole for $S_0 \rightarrow S_1$ of bathorhodopsin achieves an orientation of $\theta = 16.5^\circ$ to that of rhodopsin within 400 fs. The low initial anisotropy rising to this final bathorhodopsin value was explained either by a change in the electronic wave functions or by the presence of an absorption with low anisotropy that cancels the stimulated emission. A significant rotation of the electronic transition dipole could be occurring without the need for large nuclear displacements. Anisotropy measurements indicate that the coherent motion responsible for the oscillations of the magic-angle signal cause a less than 4° angular motion of the dipole of the product transition at 580 nm. Therefore, the motion causing the 550 fs oscillation in the absorption signals does not significantly rotate the transition dipole moment of retinal.

We also reported the first measurement of the stimulated emission signal from bovine rhodopsin, as well as a new transient absorption band at ~ 700 nm. The stimulated emission signal at 810 nm shows a rise and decay, which are instrument-response limited. The data support a multidimensional potential

energy surface that includes stretching of the carbon–carbon bonds. This introduces a coordinate faster than torsion into the retinal isomerization. Figure 6 gives a qualitative look at how we picture the excited-state surface. The traditional deactivation pathway, Figure 6, path A, involves motion from the Franck–Condon state toward the S_1/S_0 crossing along the torsion coordinate only. The deactivation proposed here, Figure 6, path B, involves initial motion from the Franck–Condon state along the carbon bond stretch coordinate followed by motion along the traditional torsion coordinate as the population approaches the S_1/S_0 crossing. This excited-state surface illustrates that stretching the carbon bonds makes the twisting motion easier. As the population crosses over into the product well, again carbon bond stretch motion accompanies the torsion to reach an equilibrated ground-state bathorhodopsin.

Acknowledgment. We thank Arie Warshel and Bob Birge for many discussions on the reaction coordinate and the potential energy surfaces for rhodopsin and Michael Robb for sending us preprints of his work. This work was supported by NIH grant GM12592 (R.M.H.), NIH NRSA postdoctoral fellowship EY06849-01 (E.A.M.), NIH grant GM35183, and NSF grant MCB-9727439 (R.H.C.) and used instrumentation developed under NIH-RR01348 (R.M.H.).

References and Notes

- (1) Birge, R. R. *Annu. Rev. Biophys. Bioeng.* **1981**, *10*, 315.
- (2) Nathans, J. *Biochemistry* **1990**, *29*, 9746.
- (3) Sakmar, T. P.; Franke, R. R.; Khorana, H. G. *Proc. Natl. Acad. Sci. U.S.A.* **1989**, *86*, 8309.
- (4) Zhukovsky, E. A.; Orian, D. D. *Science* **1989**, *246*, 928.
- (5) Kandori, H.; Katsuta, Y.; Msayoshi, I.; Sasabe, H. *J. Am. Chem. Soc.* **1995**, *117*, 2669.
- (6) Song, L.; El-Sayed, M. A.; Lanyi, J. K. *Science* **1993**, *261*, 891.
- (7) Schoenlein, R. W.; Peteanu, L. A.; Mathies, R. A.; Shank, C. V. *Science* **1991**, *254*, 412.
- (8) Peteanu, L. A.; Schoenlein, R. W.; Wang, Q.; Mathies, R. A.; Shank, C. V. *Proc. Natl. Acad. Sci. U.S.A.* **1993**, *90*, 11762.
- (9) Yan, M.; Manor, D.; Weng, G.; Chao, H.; Rothberg, L.; Jedju, T. M.; Alfano, R. R.; Callender, R. H. *Proc. Natl. Acad. Sci. U.S.A.* **1991**, *88*, 9809.
- (10) Doukas, A. G.; Junnarkar, M. R.; Alfano, R. R.; Callender, R. H.; Kakitani, T.; Honig, B. *Proc. Natl. Acad. Sci. U.S.A.* **1984**, *81*, 4790.
- (11) Kochendoerfer, G. G.; Mathies, R. A. *J. Phys. Chem.* **1996**, *100*, 14526.
- (12) Haran, G.; Wynne, K.; Xie, A.; He, Q.; Chance, M.; Hochstrasser, R. M. *Chem. Phys. Lett.* **1996**, *261*, 389.
- (13) Hasson, K. C.; Gai, G.; Anfinsen, P. A. *Proc. Natl. Acad. Sci. U.S.A.* **1996**, *93*, 15124.
- (14) Wang, Q.; Schoenlein, R. W.; Peteanu, L. A.; Mathies, R. A.; Shank, C. V. *Science* **1994**, *266*, 422.
- (15) Vreven, T.; Bernardi, F.; Garavelli, M.; Olivucci, M.; Robb, M. A.; Schlegel, H. B. *J. Am. Chem. Soc.* **1997**, *119*, 12687.
- (16) Garavelli, M.; Celani, P.; Bernardi, F.; Robb, M. A.; Olivucci, M. *J. Am. Chem. Soc.* **1997**, *119*, 6891.
- (17) Garavelli, M.; Vreven, T.; Celani, P.; Bernardi, F.; Robb, M. A.; Olivucci, M. *J. Am. Chem. Soc.* **1998**, *120*, 1285.
- (18) Warshel, A. *Proc. Natl. Acad. Sci. U.S.A.* **1978**, *75*, 2558.
- (19) Zhong, Q.; Ruhman, S.; Ottolenghi, M.; Sheves, M.; Friedman, N.; Atkinson, G. H.; Delaney, J. K. *J. Am. Chem. Soc.* **1996**, *118*, 12828.
- (20) Bonacic-Koutecki, V.; Michl, J. *Electronic Aspects of Organic Photochemistry*; John Wiley & Sons: New York, 1990.
- (21) Tallent, J. R.; Hyde, E. W.; Finsden, L. A.; Fox, G. C.; Birge, R. R. *J. Am. Chem. Soc.* **1992**, *114*, 1581.
- (22) Warshel, A. *Nature (London)* **1976**, *260*, 679.
- (23) Warshel, A.; Barboy, N. *J. Am. Chem. Soc.* **1982**, *104*, 1469.
- (24) Salem, L. *Acc. Chem. Res.* **1979**, *12*, 87.
- (25) Monger, T. G.; Alfano, R. R.; Callender, R. H. *Biophys. J.* **1979**, *27*, 105.
- (26) Kobayashi, T.; Kim, M.; Taiji, M.; Iwasa, T.; Nakagawa, M.; Tsuda, M. *J. Phys. Chem. B.* **1998**, *102*, 272.
- (27) Kandori, H.; Sasabe, H.; Nakanishi, K.; Yoshizawa, T.; Mizukami, T.; Shichida, Y. *J. Am. Chem. Soc.* **1996**, *118*, 1002.
- (28) Sension, R. J.; Repinec, S. T.; Szarka, A. Z.; Hochstrasser, R. M. *J. Chem. Phys.* **1993**, *98*, 6291.
- (29) Yoshizawa, T.; Kandori, H. Primary Photochemical Events in the Rhodopsin Molecule. In *Progress in Retinal Research*; Osborne, N. N., Chader, G. J., Eds.; Pergamon Press: Oxford, New York, Seoul, Tokyo, 1992; Vol. 11, p 33.
- (30) Kawamura, S. T. F.; Yoshizawa, T.; Sarai, A.; Kakitani, T. *Vision Res.* **1979**, *19*, 879.
- (31) Kawamura, S. W. S.; Maeda, A.; Yoshizawa, T. *Vision Res.* **1978**, *18*, 457.
- (32) Michel-Villaz, M.; Roche, C.; Chabre, M. *Biophys. J.* **1982**, *37*, 603.
- (33) Drikos, G.; Ruppel, H. *Photochem. Photobiol.* **1984**, *40*, 93.
- (34) Lewis, J. W.; Einterz, C. M.; Hug, S. J.; Kliger, D. S. *Biophys. J.* **1989**, *56*, 1101.
- (35) Cooper, A. *Nature* **1979**, *282*, 531.
- (36) Schick, G. A.; Cooper, T. M.; Holloway, R. A.; Murray, L. P.; Birge, R. R. *Biochemistry* **1987**, *26*, 2556.